

Strong metal support interaction on Co/niobia model catalysts

F.M.T. Mendes,^{a,b} A. Uhl,^a D. E. Starr,^a S. Guimond,^a M. Schmal,^b H. Kühlenbeck,^a
S. K. Shaikhutdinov,^{a,*} and H.-J. Freund,^a

^aDepartment of Chemical Physics, Fritz-Haber Institut der Max-Planck Gesellschaft, Faradayweg 4-6, 14195 Berlin, Germany

^bFederal University of Rio de Janeiro - NUCAT-PEQ-COPPE, Bl. G-128 Centro de Tecnologia, Cidade Universitária, Rio de Janeiro, Brazil

Received 5 June 2006; accepted 29 June 2006

Cobalt was deposited by physical vapor deposition onto thin well-ordered niobia films in order to model niobia supported Co catalysts. Adsorption of CO on the Co/niobia surfaces was studied by temperature programmed desorption and infrared reflection absorption spectroscopy. Structural characterization was performed by photoelectron spectroscopy and scanning tunneling microscopy. Cobalt was found to wet the niobia film and be partially oxidized at 300 K in contrast to Co deposited on thin alumina films, where three-dimensional metal particles are stable up to 600 K. The combined results clearly indicate a strong interaction of Co with the niobia surface including Co migration into the film, which may have implications for the effects of niobia observed in real catalysts.

KEY WORDS: niobia; cobalt; CO adsorption; strong metal support interaction.

1. Introduction

During last decade, niobia supported catalysts have received much attention in many important processes such as dehydrogenation of paraffins, Fischer–Tropsch synthesis, among others (see reviews [1–4]). For example, Pd and Pt catalysts supported on niobium pentoxide, Nb₂O₅, and Nb₂O₅/Al₂O₃ supports have been found to be active in propane oxidation [5] and selective to olefins in the *n*-heptane conversion [6,7]. Also, 3d-metals (Co, Ni) supported on niobia showed a higher selectivity to the high molecular weight hydrocarbons during CO hydrogenation reactions as compared to alumina and silica supported catalysts [8–11]. The effects of niobia in the supported metal catalysts are basically rationalized in terms of so called strong metal support interaction (SMSI). This interaction may provide active sites for the reaction to occur [8,9,12] but may also inhibit the reaction (see, for example [13]).

In order to understand the role of niobia in these catalysts, we have recently initiated model studies where well-defined niobium oxide films can be used as planar supports. In particular, a thin niobia film can be grown on a Cu₃Au(100) substrate [14,15]. Figure 1 schematically shows the structure of the ultra-thin film, which consists of 2/3 of a monolayer (ML) of Nb between two hexagonal O-layers, where Nb⁵⁺ cations occupy the threefold hollow sites [15]. Interestingly, this surface does not resemble any known niobia surface if the latter do not reconstruct. On the other hand, it well may be

that the “monolayer” niobia catalysts, supported on high-surface area supports such as alumina, also exhibit structures different from a simple Nb₂O₅ bulk truncation.

As the next step in our continuing studies modeling niobia supported metal catalysts, we have investigated the structure and CO adsorption properties of Co deposited on the niobia films by physical vapor deposition. The results obtained using temperature programmed desorption (TPD), infrared reflection absorption spectroscopy (IRAS), photoelectron spectroscopy (PES) and scanning tunneling microscopy (STM) clearly show a strong interaction of cobalt deposits with the niobia films at room temperature.

2. Experimental

The experiments were performed in three ultra-high vacuum (UHV) chambers denoted as “STM”, “TPD/IRAS” and “PES” (base pressure below 5×10^{-10} mbar). Each chamber was equipped with low energy electron diffraction (LEED) and a quartz crystal microbalance for calibrating the metal (Nb, Co) evaporators (Focus EFM3). The LEED patterns of the samples were used to judge the quality of the films for combining the results, obtained in different chambers.

The Cu₃Au(100) single crystal (6 mm diameter and 2 mm thick) was supplied by Mateck. The crystal temperature was controlled using a chromel–alumel thermocouple spot-welded to the edge of the crystal and a feedback control system (Schlichting Phys. Instrum). The crystal was placed between two parallel Ta wires used for resistive heating in TPD/IRAS and PES

*To whom correspondence should be addressed.
E-mail: shaikhutdinov@fhi-berlin.mpg.de

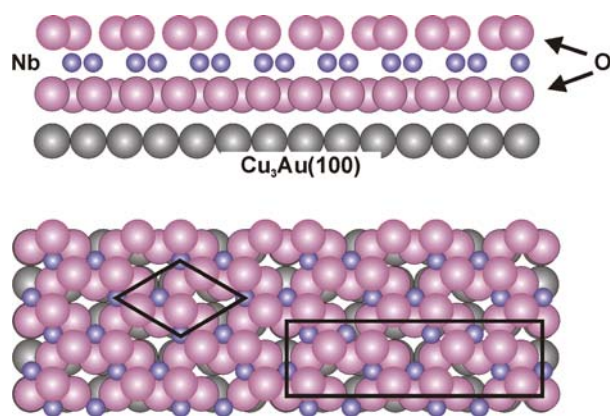


Figure 1. Cross and top views of the thin niobia film grown on $\text{Cu}_3\text{Au}(100)$. The unit cell of niobia overlayer is indicated as a rhomb. The rectangle shows the (2×7) coincidence superstructure, which is formed between oxide and metal substrate lattices. The surface shows a hexagonal lattice with a 5.3 Å periodicity.

chambers. In the STM chamber, the sample was clamped to a Mo holder and heated from the backside of the crystal using electron bombardment from a W filament.

The preparation of the niobia films has been described in details elsewhere [15]. Briefly, the clean $\text{Cu}_3\text{Au}(100)$ surface was implanted with oxygen at 300 K, using the ion sputter gun, and subsequently annealed in UHV at 650 K for 5 min. Nb was vapor deposited onto this sample kept at 300 K and then oxidized in 10^{-6} mbar O_2 at 773 K for 30 min.

Both Nb and Co were deposited in amounts presented in the paper as a nominal thickness (in Å) measured by the quartz microbalance.

For TPD measurements, the sample was placed < 1 mm far from the nozzle of a shield on a differentially pumped quadrupole mass-spectrometer (QMS) and heated at a rate of 3 K/s. IRAS experiments were

performed with a Bruker IFS 66vs spectrometer (resolution $\sim 2 \text{ cm}^{-1}$) at grazing incidence (83° with respect to the surface normal). STM measurements were performed at room temperature with Omicron Micro-H microscope.

3. Results and discussion

First we have studied the adsorption of CO on the clean niobia films in order to discriminate between CO adsorbing on the Co deposits and the niobia film support. In addition, it is well documented that CO is a good probe molecule for characterization of Lewis acid sites on oxide surfaces [16,17] that may help in further understanding of the surface structure of the niobia film.

3.1. CO adsorption on the thin niobia film

Figure 2(a) presents typical CO TPD spectrum observed for thin niobia films. Three desorption peaks at 125, 155 and 272 K are clearly seen. The spectrum for the clean $\text{Cu}_3\text{Au}(100)$ substrate is also shown, for comparison. The O-implanted $\text{Cu}_3\text{Au}(100)$ surface, treated at the same conditions as for preparation of the niobia films, was essentially inert towards CO. Therefore, the TPD signals observed on the niobia films can be definitely assigned to CO adsorption on the niobia surface. Consecutively measured spectra were identical and did not show any CO_2 formation, indicating that the niobia film does not suffer from reduction by CO under these conditions and that CO molecularly adsorbs on the niobia films. The highest desorption temperature observed (~ 270 K) is unusually high since CO usually desorbs from the various oxide surfaces at temperatures below 200 K [18]. This state cannot be assigned to metallic Nb species since CO desorbs from metallic Nb surfaces at ~ 425 K [19].

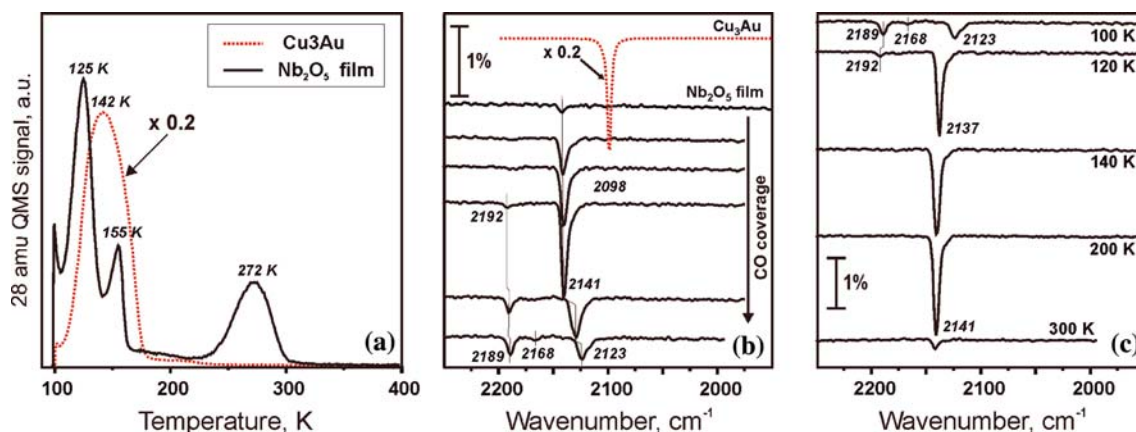


Figure 2. (a) Typical TPD spectrum of CO adsorbed on thin niobia films at 100 K. (b) IRAS spectra of CO adsorbed on thin niobia films as a function of CO exposure at 100 K. (c) IRAS spectra of CO adsorbed at 100 K and subsequently flashed to the indicated temperatures. All spectra are recorded at 100 K. The TPD and IRAS spectra for a $\text{Cu}_3\text{Au}(100)$ substrate at saturation CO coverage are also shown in (a) and (b), for comparison.

The results of the complementary IRAS study are shown in figure 2(b,c). The spectrum obtained for the clean $\text{Cu}_3\text{Au}(100)$ surface is also shown, for comparison. A strong absorption band observed at 2098 cm^{-1} on $\text{Cu}_3\text{Au}(100)$ is typical for atop CO species on metals [20]. It is blue-shifted with respect to CO on $\text{Cu}(100)$ (2072 cm^{-1} [21]) due to the presence of gold weakening the CO–Cu bond (cf. $T_{\text{des}} \sim 200\text{ K}$ for $\text{Cu}(100)$ [22] and 142 K for $\text{Cu}_3\text{Au}(100)$).

On the niobia films, the signal at 2141 cm^{-1} first gains intensity with increasing CO exposure, but then attenuates and shifts to 2123 cm^{-1} . Simultaneously, a small signal at 2192 cm^{-1} emerges which grows and shifts to 2189 cm^{-1} at saturating CO coverage, where one more peak at 2168 cm^{-1} appears. (Note, that the signals at ~ 2120 and 2165 cm^{-1} were also observed on these films at elevated (ca. 10^{-6} mbar) CO pressures in a gas phase using a SFG technique [23]). The coverage dependence of the main peak at $2141\text{--}2123\text{ cm}^{-1}$ is typical for the systems with a strong CO–CO interaction and can be rationalized on the basis of redistribution of the adsorption sites with increasing CO coverage [24].

Figure 2(c) shows IRAS spectra of CO adsorbed at 100 K after thermal flash to the specified temperatures and cooling back to 100 K . CO species with the stretching frequency of ~ 2190 and 2168 cm^{-1} desorb at 140 K , which correlates well with the TPD peak at 125 K . Heating to 200 K results only in small increase of the peak intensity at 2141 cm^{-1} , indicating that CO species resulted in the TPD peak at 155 K are IR inactive. The most prominent peak at 2141 cm^{-1} disappears only upon further heating to 300 K , thus indicating that these species are associated with CO TPD signal at 272 K .

It is important to note that the integrated TPD area of CO desorbing from the niobia films is about five times smaller, on average, than from the clean $\text{Cu}_3\text{Au}(100)$ surface. Since the CO saturation coverage on $\text{Cu}_3\text{Au}(100)$ at 100 K is about 0.3 ML [24], the amounts of CO adsorbed on the niobia surface is calculated to be less than 0.2 molecules per Nb_2O_5 unit cell (see figure 1). On the other hand, as mentioned above, the CO coverage dependence of the IRAS spectra in the $2141\text{--}2123\text{ cm}^{-1}$ range (see figure 2) indicates a strong CO–CO interaction. Bearing in mind, that the thin niobia film is oxygen terminated as shown in figure 1, it appears that CO does not adsorb on the regular surface but on some extended defects present in the film where a local CO concentration can be relatively high which may in turn explain a strong CO–CO interaction observed. For example, the ill-defined boundaries between niobia domains as observed by STM [15] could be responsible for this.

CO is generally considered as a probe molecule for the Lewis acid sites on oxides [16,17]. Owing to the Pauli repulsion between carbon lone-pair electrons and the surface charge distribution, adsorbed CO seems to

vibrate against a rigid wall (so called “wall effect”). As a result, the CO stretching frequency is shifted to higher wavenumbers compared to the gas phase value (2143 cm^{-1}). However, metal cations which contain partially filled d-orbitals can interact with the $2\pi^*$ -orbital of CO via electron back-donation from the metal to CO thus lowering the vibrational frequency [25]. For example, the CO stretching frequency on Co^{2+} in CoO 2118 cm^{-1} is much lower than for Co^{3+} in Co_3O_4 2175 cm^{-1} [16,17].

On silica supported N_2O_5 particles, Knözinger and co-workers observed the signal at 2191 cm^{-1} (i.e. blue-shifted with respect to CO in the gas phase) which was assigned to CO bonded to Nb^{5+} surface atoms [26]. Therefore, the weak signal at $2189\text{--}92\text{ cm}^{-1}$ observed on the niobia films can be assigned to the adsorption on the Nb^{5+} cations. Concomitantly, the most prominent peak at 2141 cm^{-1} can be associated with Nb species, which are partially reduced and thus contain d-electrons through which Nb interacts more strongly with CO via back-donation effect. For example, step edges of the niobia terraces and domain boundaries can in principle expose low coordinated and partially reduced Nb cations, which may adsorb CO much stronger than regular terrace sites.

3.2. Structure and CO adsorption properties of Co on the niobia films

Figure 3 shows STM images of Co deposited at 300 K on the niobia films at two Co coverages, 0.5 \AA (a) and 2 \AA (c), respectively. It is clear that small particles are homogeneously dispersed on the surface and coalesce at higher coverage. However, the majority of these particles are only $1.5\text{--}2\text{ \AA}$ in height. This implies that Co essentially wets the surface and forms two-dimensional, monolayer islands at 300 K . Since the formation of these islands can be kinetically limited, we have examined the surface after annealing to 500 K , which resulted in large well-shaped monolayer islands at low Co coverage (figure 3c). At high Co coverage, the ill-defined and relatively rough surface, with a corrugation amplitude of ca. 1 \AA , is observed in figure 3(d). Note, that this morphology is very different from Co deposited on thin alumina films, where three-dimensional particles up to 2 nm in height are formed under these conditions [27].

Figure 4(a) shows CO TPD spectra measured for $\sim 1\text{ \AA}$ Co deposited on the niobia film at 100 K . The first TPD run showed several desorption signals at around 150 , 275 , 340 and 400 K . Basically, the CO desorption at $250\text{--}450\text{ K}$ is characteristic for the metallic Co particles as shown in the same figure for the Co particles deposited on the thin alumina films. The signal centered at 387 K has been previously assigned to atop CO species, and the shoulder at 275 K to the depopulation of $\text{Co}(\text{CO})_n$ species [28].

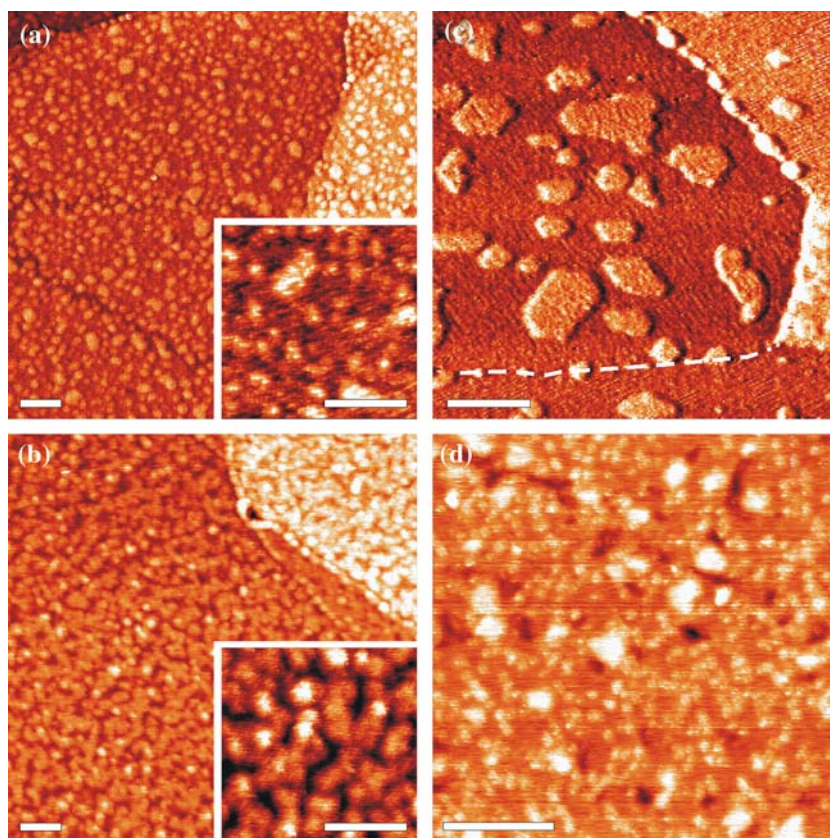


Figure 3. STM images of Co deposited at 300 K on thin niobia films. The Co coverage is 0.5 Å (a and c) and 2 Å (b and d). Images (c) and (d) are taken after heating the same samples to 500 K. The scale bar corresponds to 20 nm. Tunneling parameters are: (a) bias 1.2 V, current 1 nA; (b) 0.75 V, 0.7 nA; (c) 1.25 V, 1.3 nA; (d) 0.75 V, 1 nA. Image (c) is presented in differentiated contrast, where the domain boundary is marked by the dash line.

However, the second CO TPD spectrum on the Co/niobia sample is in fact very similar to that for the clean niobia film, except the small feature at around 180 K. Meanwhile, the CO TPD experiments on alumina supported Co particles revealed only minor changes in the repeated spectra (not shown here). This finding clearly shows that significant structural changes occur upon heating of the Co/niobia surface. Interestingly, when Co was additionally deposited on top of the same sample, the situation repeated itself: the desorption signals from metallic cobalt vanished after heating to 500 K.

Surprisingly, Co deposition at 300 K did not result in TPD feature that could be associated with the metallic Co surface (see figure 4b). The spectrum appears similar to the clean niobia film with an additional signal at around 200 K (compare figures 2a and 4b). Therefore, the TPD results show that Co strongly interacts with the niobia films at room temperature leading to losing metallic properties of the Co deposits.

Since CO desorption and structural changes occur on heating simultaneously, this may affect a TPD spectrum. In order to monitor CO adsorption as a function of temperature we have measured IRAS spectra of 10 L of CO adsorbed at 100 K after stepwise heating to the elevated temperatures as shown in figure 4(c,d).

For the case of Co deposited at 100 K (see figure 4c), the absorption band centered at 2082 cm^{-1} is observed, which is similar to the spectra reported for the Co/alumina system and can be assigned to $\text{Co}(\text{CO})_n$ species [28]. Upon heating to 300 K, the spectrum is altered such that several species can be resolved (at 2050 , 2078 and 2098 cm^{-1}) which are gradually attenuated at higher temperatures due to CO desorption. Another peak, observed at 2127 cm^{-1} at 100 K, shifts to 2135 cm^{-1} and increases in intensity upon heating to 140 K, but disappears at 300 K like on the clean niobia films (see figure 2c). Therefore this species can be assigned to CO adsorbed on defect sites of the niobia film implying that Co does not preferentially nucleate on the defects.

Adsorption of CO at 100 K on the sample heated to 500 K showed basically only one band at 2187 cm^{-1} (a weak signal at 2125 cm^{-1} can be assigned to the niobia film) which is consistent with strong structural changes upon heating as observed by TPD. Interestingly, this signal emerges from the beginning for Co deposited at 300 K as shown in figure 4(d), while the signals at 2135 and 2086 cm^{-1} are similar to those observed for Co deposited at 100 K, much weaker though. Upon heating to 300 K, no IR signals are

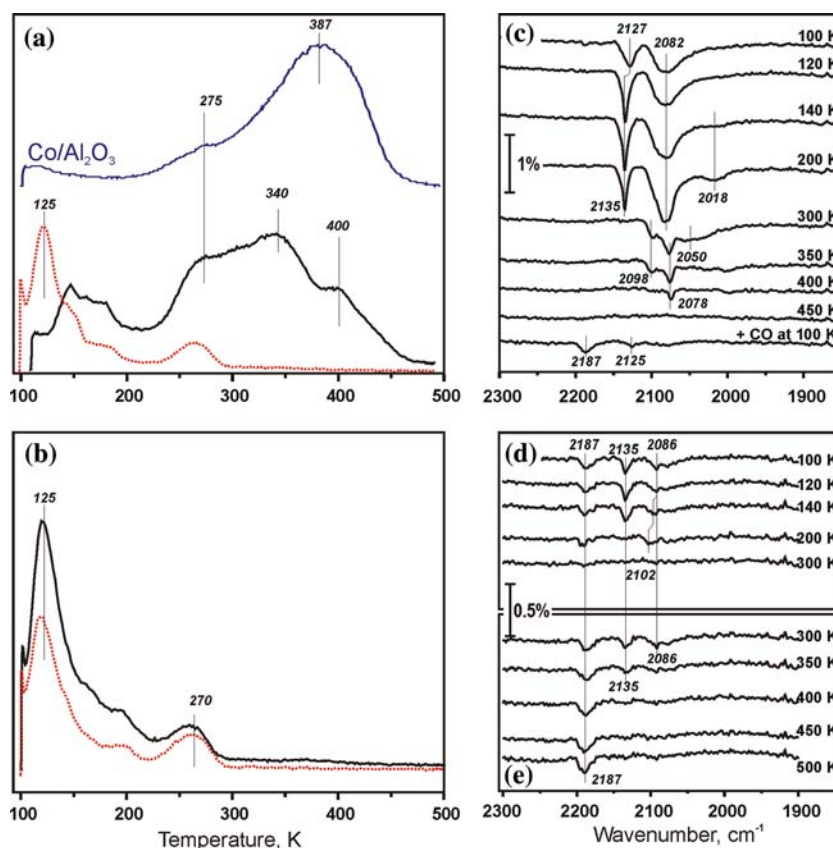


Figure 4. (a and b) First (solid) and second (dotted) TPD spectra of 10 L of CO adsorbed on $\sim 1 \text{ \AA}$ Co deposited on thin niobia films at 100 K (a) and 300 K (b). Typical CO TPD spectrum for Co on thin alumina film (offset for clarity) is also shown, for comparison. (c) CO IRAS spectra of Co deposited on niobia at 100 K and recorded at 100 K after heating to the indicated temperature. (d) CO IRAS spectra of Co deposited on niobia at 300 K and recorded at 100 K after heating to the indicated temperature. Image (e) shows the spectra of sample (d) when 10 L of CO was adsorbed at 100 K after the sample was flashed to the indicated temperatures.

observed, which is consistent with the complete CO desorption as shown by TPD in figure 4(b). Figure 4(e) shows that heating to the higher temperatures and subsequent CO adsorption at 100 K basically leads to vanishing of IR bands except at 2187 cm^{-1} . Therefore, independently of the Co deposition temperature, annealing to 500 K results in the only CO species at 2187 cm^{-1} . This frequency is very close to that observed on the clean niobia film (2189 cm^{-1} , see figure 2), which has been assigned to CO adsorbed on Nb^{5+} cations. Therefore, the results indicate that niobia encapsulates the Co deposits such that the resulting surface loses the metallic adsorption properties.

The electronic structure of the Co species on the niobia films was studied by PES using synchrotron radiation. Figure 5 shows PES spectra before and after Co deposition at 300 K. The clean film is characterized by the binding energies (BE) of the Nb $3d_{5/2}$ level at 206.4 eV and of the O 1s level at 529.8 eV. Note, that the BE of the Nb level is $\sim 0.6 \text{ eV}$ lower than for Nb^{5+} in Nb_2O_5 powders ($\sim 207 \text{ eV}$ [29]) due to the well-documented screening effect of the metal substrate underneath oxide films.

For Co deposited at 300 K the PE-spectra show two species characterized by BE of Co $2p_{3/2}$ at 778 and 781 eV. These values are typical for metallic (Co^0) and oxidized ($\text{Co}^{\delta+}$, like in Co_3O_4 or CoO) states, respectively [30]. The $\text{Co}^{\delta+} : \text{Co}^0$ integral ratio increases from 0.1 to 0.3 when the spectrum is measured at grazing incidence. This indicates that $\text{Co}^{\delta+}$ species are on the surface, while metallic Co is mostly located in the sub-surface region. In principle, this could be explained by the formation of the Co particles with oxidized $\text{Co}^{\delta+}$ species on the surface modified by Nb^{5+} as revealed by CO IRAS. However, the STM images presented in figure 3 did not show the three-dimensional particles but single layer islands, which are typical for the morphology of metal-on-metal systems. Therefore, it seems likely that Co migrates through the film and forms a metallic layer directly bonded to the $\text{Cu}_3\text{Au}(100)$ substrate. In this model, the oxidized $\text{Co}^{\delta+}$ species are formed on or incorporated into the niobia film, thus resulting in a partial reduction of the niobium cations. The formation of two Nb species is clearly seen in the Nb3d spectrum of the Co/niobia sample, which splits into two components, centered at 207.1 and 206.2 eV for the Nb $3d_{5/2}$

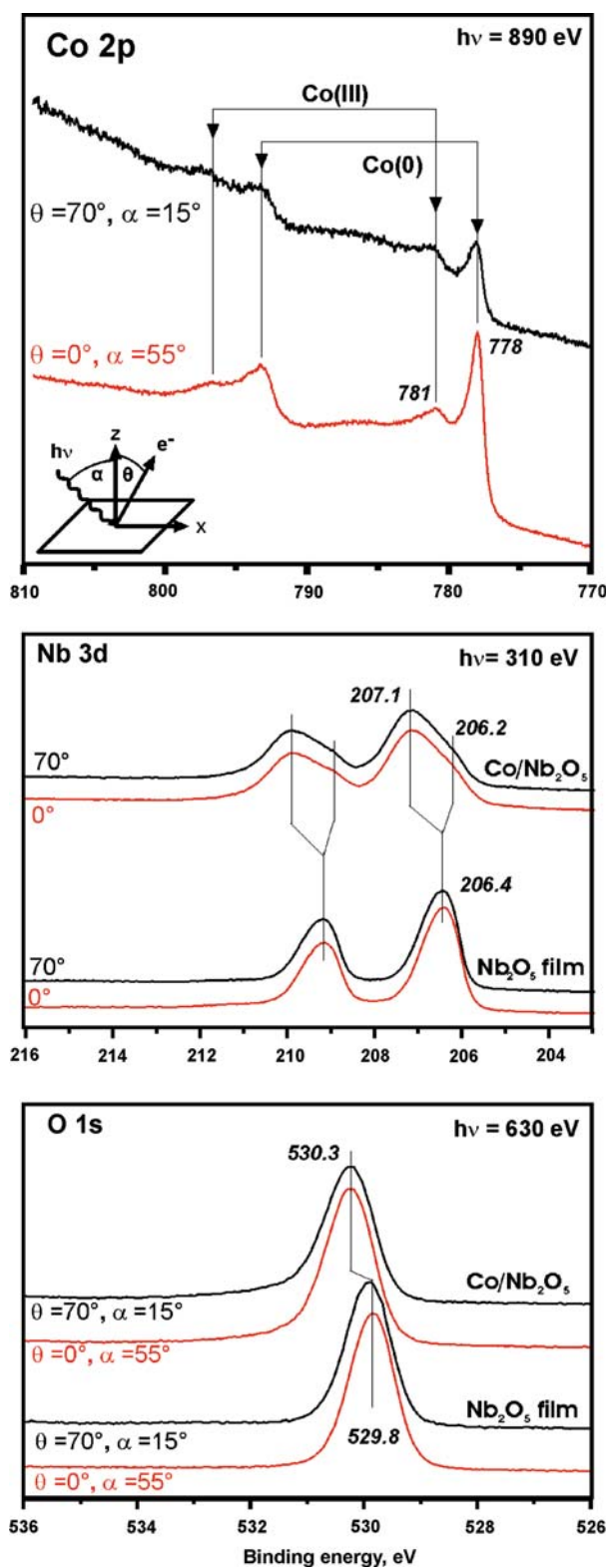


Figure 5. Co2p, Nb3d and O1s regions of photoelectron spectra measured at two different geometries as depicted in the inset. The spectra for Nb and O core levels are shown before and after 2 Å of Co have been deposited at 300 K.

level, (after deconvolution not shown here). The ratio between these two signals does not depend on the detection angle as shown in figure 5, which suggests that

all Nb species lie in a single layer as in the original film (see figure 1). The component at 207.1 eV deserves a comment since the binding energy is higher than in the original niobia film, where Nb is already in its highest oxidation state, 5+. We tentatively attribute this effect to the presence of cobalt ions and reduced niobia ions in the film, which probably pin the Fermi level at a different position.

Although the precise structure of this mixed Co–Nb oxide phase needs further studies, the PES results clearly show that Co deposited on the niobia film can be readily oxidized at room temperature, which is in contrast to Co deposits on the alumina films [27,28].

4. Summary

We have studied the structure and CO adsorption properties of cobalt vapor deposited onto thin well-ordered niobia films as niobia supported Co model catalysts. The combined TPD, IRAS and PES results show that Co deposits on the niobia film can be readily oxidized at room temperature. The metallic Co phase can be stabilized on the niobia surface only by deposition at low temperatures due to kinetic limitations. The Co–niobia interaction leads to the mixed Co–Nb oxide structure where the surface may expose Nb^{5+} species as observed by CO IRAS. In addition, the Co species may migrate through the film, more efficiently at elevated temperatures, and therefore be directly bonded to the Cu_3Au substrate. Preliminary results show that this effect is not caused by the small thickness of the niobia film studied: For the thicker films, the Co deposits are found to lose the metallic properties upon heating to 500 K as well. These results are in large contrast to Co deposited on the thin alumina films, where three-dimensional metal particles are formed at 300 K and remain stable up to 600 K [27,28]. These results could shed light on the promotional effect of niobia, observed on the real niobia supported Co catalysts, whose exceptional catalytic properties are rationalized on the basis of the SMSI effect [8,9].

Acknowledgments

We acknowledge support from the Fonds der Chemischen Industrie and Deutsche Forschungsgemeinschaft through SFB 546. F.M.T. Mendes and M. Schmal acknowledge the financial support from Coordenação de Aperfeiçoamento de Pessoal de Nível Superior, CAPES-Brasil (Grant-BEX2454/03–3).

References

- [1] I. Nowak and M. Ziolk, Chem. Rev. 99 (1999) 3603.
- [2] K. Tanabe, Catal. Today 78 (2003) 65.

- [3] M. Ziolek, *Catal. Today* 78 (2003) 47.
- [4] I.E. Wachs, *Catal. Today* 100 (2005) 79.
- [5] F.B. Noronha, D.A.G. Aranda, A.P. Ordine and M. Schmal, *Catal. Today* 57 (2000) 275.
- [6] M. Schmal, D.A.G. Aranda, R.R. Soares, F.B. Noronha and A. Frydman, *Catal. Today* 57 (2000) 169.
- [7] F.B. Passos, D.A.G. Aranda and M. Schmal, *Catal Today* 57 (2000) 283.
- [8] F.M.T. Mendes, C.A.C. Perez, F.B. Noronha, C.D.D. Souza, D.V. Cesar, H.-J. Freund and M. Schmal, *J. Phys. Chem. B* 110 (2006) 9155.
- [9] F.M.T. Mendes, C.A. Perez, F.B. Noronha and M. Schmal, *Catal. Today* 101 (2005) 45.
- [10] T. Iizuka, Y. Tanaka and K. Tanabe, *J. Mol. Catal.* 17 (1982) 381.
- [11] E.I. Ko, M. Hupp and K. Fogar, *J. Catal.* 86 (1984) 315.
- [12] A.C. Faro, P. Grange and A.C.B. dos Santos, *Phys. Chem. Chem. Phys.* 4 (2002) 3997.
- [13] A. Jasik, R. Wojcieszak, S. Monteverdi, M. Ziolek and M.M. Bettahar, *J. Mol. Catal. A* 242 (2005) 81.
- [14] J. Middeke, R.-P. Blum and H. Niehus, *Surf. Sci.* 587 (2005) 219.
- [15] D.E. Starr, F.M.T. Mendes, J. Middeke, R.-P. Blum, H. Niehus, D. Lahav, S. Guimond, A. Uhl, T. Kluener, M. Schmal, H. Kuhlbeck, S. Shaikhutdinov and H.-J. Freund, *Surf. Sci.* 599 (2005) 14.
- [16] A. Zecchina, D. Scarano and S. Bordiga, *Catal. Today* 27 (1996) 403.
- [17] A.A. Davydov, *Infrared Spectroscopy Of Adsorbed Species on the Surface of Transition Metal Oxides* (Wiley, 1984).
- [18] H. Kuhlbeck, H.-J. Freund, *Landolt-Börnstein NewSeries* (Springer-Verlag, 2006).
- [19] A.L. Cabrera and J. Espinosa-Gangas, *J. Mater. Res.* 17 (2002) 2698.
- [20] P. Hollins, *Surf. Sci. Rep.* 16 (1997) 51.
- [21] J.C. Cook and E.M. McCash, *Surf. Sci.* 371 (1997) 213.
- [22] S. Vollmer, G. Witte and C. Wöll, *Catal. Lett.* 77 (2001) 97.
- [23] F. Höbel, A. Bandara, G. Rupprechter and H.-J. Freund, *Surf. Sci.* 600 (2006) 963.
- [24] G.W. Graham, *Surf. Sci.* 187 (1987) 490.
- [25] G. Blyholder, *J. Chem. Phys.* 68 (1964) 2772.
- [26] T. Beutel, V. Siborov, B. Tesche and H. Knözinger, *J. Catal.* 167 (1997) 379.
- [27] T. Hill, M. Mozaffari-Afshar, J. Schmidt, T. Risse, S. Stempel, M. Heemeier and H.-J. Freund, *Chem. Phys. Lett.* 292 (1998) 524.
- [28] A.F. Carlsson, M. Bäumer, T. Risse and H.-J. Freund, *J. Chem. Phys.* 119 (2003) 10885.
- [29] D. Morris, Y. Dou, J. Rebane, C.E.J. Mitchell, R.G. Egdell, D.S.L. Law, A. Vittadini and M. Casarin, *Phys. Rev. B* 61 (2000) 13445.
- [30] XPS and AES Database, Thermo Electr. Corp. <http://www.la-surface.com/database/element.php>.